RF Limiter Metamaterial Using p-i-n Diodes

Alexander R. Katko, *Student Member, IEEE*, Allen M. Hawkes, John P. Barrett, *Student Member, IEEE*, and Steven A. Cummer, *Fellow, IEEE*

(Invited Paper)

***Abstract*—We present the design and experimental implementation of an RF limiter metamaterial using a sheet of nonlinear metamaterials. We demonstrate that complementary electric inductive-capacitive resonators loaded with nonlinear p-i-n diodes can act as RF limiter unit cells. We design and fabricate limiter metamaterials and compare them to traditional circuit limiters. Our limiter metamaterial exhibits a minimum insertion loss under 3 dB, a maximum decrease in transmission of 6.95 dB and broadband performance, with a minimum decrease in transmission of 3 dB over 18% bandwidth. The limiter metamaterial is suitable for a wide variety of practical applications requiring protection of sensitive devices from high power.**

***Index Terms*—Metamaterials, nonlinear metamaterials, RF limiter.**

I. Introduction

METAMATERIALS are subwavelength structures designed such that their electromagnetic properties are different than the electromagnetic properties of their constituent materials. Metamaterials can be used to design effective materials with exotic properties not found in nature. These properties can range from a negative index of refraction [1] to a zero index of refraction [2]. Many interesting applications of metamaterials have been devised, ranging from an invisibility cloak (e.g., [3]) to absorbers [4], [5]. Linear metamaterial structures have been used to create these and other devices. The use of nonlinear metamaterials to achieve interesting effects has not been explored to the same extent as that of linear metamaterials. Nonlinear metamaterials have been used to demonstrate shifting of a resonant frequency [6], [7], harmonic generation [8], mixing [9], and phase conjugation [10]. However, many other possible applications have not been explored to this point.

II. RF Limiter

Metamaterials offer the potential of having a circuit function realized by a sheet of material or even a volume. One particular RF device of interest is a limiter. An RF limiter has a variable output power depending on the input power. An ideal limiter has the following characteristics:

$$P_{\rm out} = P_{\rm in}, P_{\rm in} < P_{\rm t} \tag{1}$$

$$P_{\rm out} = P_{\rm t}, P_{\rm in} > P_{\rm t} \tag{2}$$

where $P_{\rm t}$ is a specified threshold power. A realistic limiter will exhibit some insertion loss, signified by a downward shift in the $P_{\rm out}$ versus $P_{\rm in}$ curve. $P_{\rm out}$ for a realistic limiter also increases with increasing $P_{\rm in}$ even above $P_{\rm t}$. To illustrate the characteristics of a realistic limiter, we show $P_{\rm out}$ versus $P_{\rm in}$ curves in Fig. 1 for a traditional circuit limiter. The dashed-dottted curve represents a generic linear, impedance-matched device: $P_{\rm out} = P_{\rm in} - L_{\rm in}$, where $L_{\rm in}$ is the insertion loss. The dashed curve represents the ideal nonlinear limiter with small insertion loss: For $P_{\rm in} \geq P_{\rm t}$, $P_{\rm out} = P_{\rm t} - L_{\rm in}$. The solid curve shows measured data from a traditional circuit limiter to illustrate the differences between ideal and realistic limiters: Realistic limiters exhibit a bowing at the "knee" (the threshold power level). Above $P_{\rm t}$, there is still some dependence on $P_{\rm in}$. We define the limiter's isolation ΔS_{21} as

$$\Delta S_{21} \equiv S_{21,\text{low-power}} - S_{21,\text{high-power}}. \tag{3}$$

The circuit limiter was also measured to establish a baseline. Our proposed limiter metamaterial is a material suitable for use in a waveguide or free-space system. To our knowledge, nonlinear limiter materials suitable for such systems have not been demonstrated, so there is no direct comparison to our proposed metamaterial. Our metamaterial is also not a traditional circuit

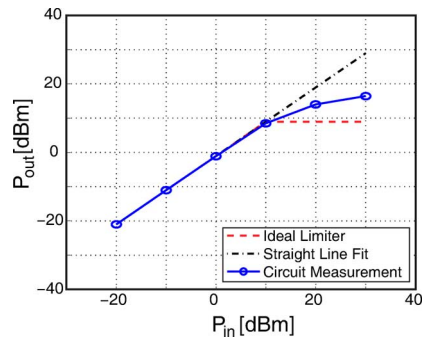

Fig. 1. Illustrative $P_{\rm out}$ versus $P_{\rm in}$ characteristics for several cases. The first case (dashed-dotted curve) is a generic linear device with some small insertion loss. The dashed curve represents an ideal RF limiter. The solid curve is a realistic circuit limiter used to illustrate the differences between ideal and implementable limiters.

Manuscript received October 15, 2011; revised December 16, 2011; accepted December 19, 2011. Date of publication January 02, 2012; date of current version January 30, 2012. This work was supported in part by DARPA under Contract No. HR0011-05-C-0068 and a Lockheed Martin University Research Initiative.

The authors are with the Department of Electrical and Computer Engineering and Center for Metamaterials and Integrated Plasmonics, Duke University, Durham, NC 27708 USA (e-mail: cummer@ee.duke.edu).

Color versions of one or more of the figures in this letter are available online at http://ieeexplore.ieee.org.

Digital Object Identifier 10.1109/LAWP.2011.2182490

limiter. Thus, we compare our waveguide or free-space limiter metamaterial to a conventional coplanar waveguide limiter to establish the nonlinear performance characteristics of a conventional limiter as the closest related technology even though the metamaterial is intrinsically not a conventional circuit limiting device.

The primary characteristics of interest for a limiter are the insertion loss; the 3-dB isolation bandwidth, defined as the bandwidth corresponding to $\Delta S_{21} \geq 3$ dB; and the maximum isolation, defined as the maximum of ΔS_{21} for a given frequency. These are the metrics we use to compare our limiter metamaterial to a circuit limiter. Ideally, a limiting device or material should have high isolation over a wide bandwidth with low insertion loss. High isolation is required to approach the dashed curve in Fig. 1.

A limiter is typically used to protect sensitive devices from very high incident power levels, such as a low noise amplifier (LNA). Limiters are often implemented using p-intrinsic-n (p-i-n) diodes in various configurations. A p-i-n diode can be modeled as a series resistance $R_{\rm s}$ and a series capacitance. The series resistance as a function of the bias current I_D is given by

$$R_{\rm s} = \frac{R_{\max} A}{A + R_{\max} I_D^k} + R_{\min} \tag{4}$$

where $R_{\max}$ is the maximum resistance, A and k are fitting parameters based on the particular diode used, and $R_{\min}$ is the minimum resistance. As the incident power $P_{\rm in}$ and thus I_D increase as $R_{\rm s}$ decreases. A circuit limiter using p-i-n diodes usually connects the p-i-n diode or diodes in shunt to ground. At low $P_{\rm in}$, the p-i-n presents a high impedance, while at high $P_{\rm in}$, it presents a low impedance, effectively shorting the circuit's load and preventing $P_{\rm out}$ from increasing once $P_{\rm in}$ reaches some threshold. Using two p-i-n diodes in parallel with reverse polarities allows this function for both half-cycles of a period, providing a simple and effective limiter circuit.

We choose to implement an analog to this circuit suitable for free-space or waveguide applications through the use of metamaterials. The p-i-n diode selected for this work is an Avago Technologies HSMP-3822, a device with a thin intrinsic region that is particularly suited for low-$P_{\rm t}$ limiters.

III. Design and Simulation

The base metamaterial particle selected to perform the aforementioned circuit functions is a complementary electric inductive-capacitive (CELC) resonator [11]. A CELC is a planar metamaterial and thus well suited for constructing an RF limiter sheet. As the complement of an ELC resonator, a CELC exhibits high reflection except at its resonant frequency f_0, while exhibiting high transmission at f_0. The p-i-n diodes are used to short the interiors of the CELCs at high power, preventing them from resonating and thus decreasing transmission. We designed the CELCs to resonate above 2.5 GHz in simulation because the addition of the p-i-n diode capacitance depresses f_0. The lattice size was 17 mm, and the dielectric footprint was 15 mm. The exposed dielectric traces were 1 mm wide, with a complementary gap of 0.5 mm. A particle with these dimensions resonated at $f_0 \approx 3$ GHz when loaded with a lumped resistor and capacitor equivalent to a p-i-n diode. The actual capacitance of the p-i-n diodes used was higher than the specification, which is why f_0 is lower in our measurements than in simulations.

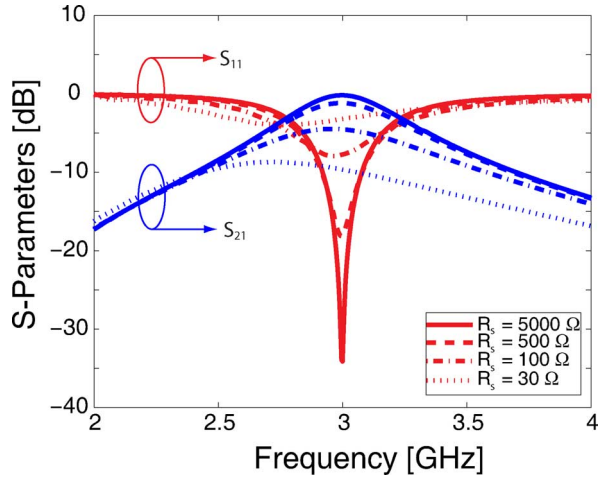

Fig. 2. *(color online)* Simulated S-parameters for array of p-i-n-loaded CELCs. The red set of curves is S_{11} for varying $R_{\rm s}$. The blue set of curves is S_{21} for varying $R_{\rm s}$. Solid curves correspond to low bias current (low incident power), and dotted curves correspond to high bias current (high incident power).

To model the CELC circuit, we used CST Microwave Studio to simulate a CELC array loaded with lumped element impedances that approximate the characteristics of the p-i-n diodes at varying bias levels. Using (4) for our particular p-i-n diodes, $R_{\rm s}$ varies between approximately 5000 and 30 Ω. Our p-i-n diodes also had a specified maximum capacitance of 0.8 pF. The simulated S-parameters for various $R_{\rm s}$ values in this range are shown in Fig. 2.

These simulations show that as $R_{\rm s}$ decreases (corresponding to increasing $P_{\rm in}$), S_{21} decreases near f_0. The metamaterial is clearly functioning as a limiter. For these simulations, the isolation is over 10 dB, and the 3-dB isolation bandwidth is over 40%.

A traditional circuit limiter was designed and fabricated using a coplanar waveguide (CPW) transmission line. Although our limiter metamaterial is not a traditional transmission-line-based device, a traditional limiter provides the closest technology for comparison.

The limiter metamaterial was then designed and fabricated to resonate at 2.5 GHZ. Both a single CELC limiter metamaterial and a 4×2 array of CELC limiter metamaterials were fabricated for testing inside a closed rectangular waveguide. The measurement setup for the single CELC limiter metamaterial and array limiter metamaterial was the same, while the CPW circuit limiter was tested using direct SMA connections.

We mounted both to metal sheets in order to ensure a good electrical connection with the waveguide. The single CELC limiter metamaterial is shown in Fig. 3(a), and the CELC array limiter is shown in Fig. 3(b).

IV. Experiment

Both the CPW circuit limiter and the CELC limiter metamaterials were tested utilizing a vector network analyzer (VNA). In order to characterize the samples under high incident power,

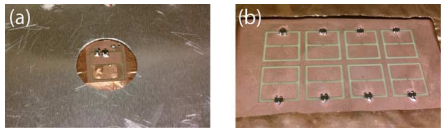

Fig. 3. Photographs of fabricated PIN-CELC limiter metamaterials. (a) Single CELC mounted on aluminum sheet for testing. (b) Array of CELCs mounted on copper sheet for testing. p-i-n diodes are visible on both.

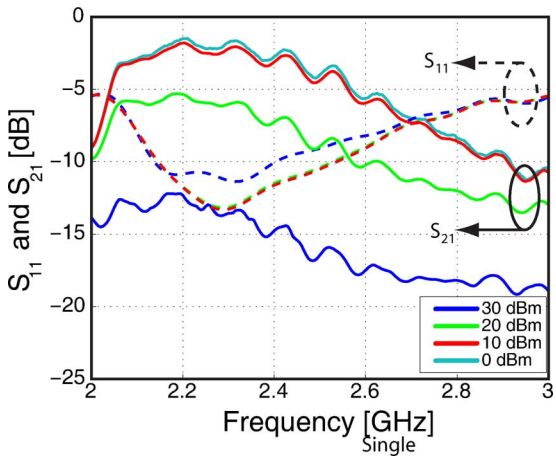

Fig. 4. Measured S-parameters as functions of $P_{\rm in}$ for CPW circuit limiter. Solid curves are S_{21}; dashed curves are S_{11}. $P_{\rm in}$ levels are shown.

a power amplifier was used. Attenuators were also used to avoid damage to the VNA. The maximum nominal incident power available to the CELCs was approximately +30 dBm.

S_{11} measurements were also conducted without the amplifier or attenuator in place in order to calibrate the full measurements. Without the amplifier, the maximum nominal incident power available to the CELCs was approximately +10 dBm. The CPW limiter was tested as a baseline for the isolation, bandwidth, and insertion loss. Using the measured S-parameters, we can extract $P_{\rm out}$ versus $P_{\rm in}$ for the test samples.

The measured S-parameters for the CPW limiter are shown in Fig. 4.

The CPW device functions as expected, exhibiting much lower transmission for high $P_{\rm in}$. The maximum isolation for the CPW limiter, as shown in Fig. 4, is approximately 12.9 dB for $P_{\rm in}$ varying from 0 to +30 dBm. The p-i-n diode itself is also very broadband, with approximately 37.8% 3-dB isolation bandwidth, so any bandwidth limitations should be due to the CELCs themselves. The minimum insertion loss for the CPW limiter is 1.036 dB. This is expected given the direct cable connections and use of an impedance-matched CPW transmission line.

With this baseline, we tested the single CELC unit cell (mounted to the aluminum sheet) and the CELC array. S_{11} is shown for both the single CELC and array in Fig. 5, and S_{21} is shown for both the single CELC and array in Fig. 6.

The maximum isolation for the single CELC is 11.8 dB for the same $P_{\rm in}$ variation as the CPW circuit limiter with a 3-dB isolation bandwidth of 16.4%. The maximum isolation is very close to that of the circuit limiter. While the 3-dB isolation bandwidth is smaller than that of the circuit limiter, it is still very broadband. However, the low-$P_{\rm in}$ minimum insertion loss of 10.2 dB

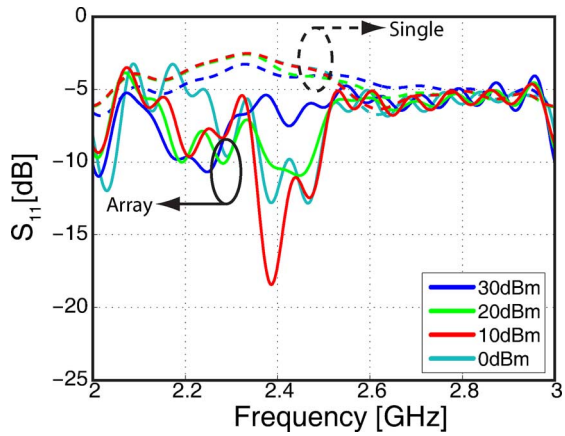

Fig. 5. Experimental S_{11} as function of $P_{\rm in}$ for both the single and array CELC limiter metamaterials. Solid curves are the array; dashed curves are the single CELC. The array limiter metamaterial has lower return loss than the single CELC limiter metamaterial. $P_{\rm in}$ levels are shown for both curves.

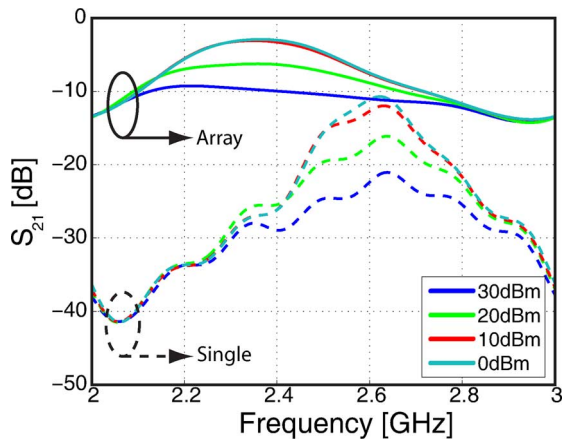

Fig. 6. Experimental S_{21} as function of $P_{\rm in}$ for both the single and array CELC limiter metamaterials. Solid curves are the array; dashed curves are the single CELC. The array limiter metamaterial has much lower insertion loss than the single CELC limiter metamaterial, although the single CELC limiter metamaterial has higher isolation. $P_{\rm in}$ levels are shown for both curves.

for the single CELC is much higher. This is expected due to the aluminum mounting sheet: Most of the cross section of the waveguide is taken up by aluminum rather than the resonant CELC. Consequently, the transmission should be much higher for the full CELC array since there is no solid metal sheet filling the waveguide.

The maximum isolation ΔS_{21} for the CELC array is 6.95 dB for the same $P_{\rm in}$ variation as the previous tests. However, the minimum insertion loss at low $P_{\rm in}$ is 2.7 dB, significantly better than the single CELC and approaching that of the CPW limiter. The performance is also very broadband, with a 3-dB isolation bandwidth of 18%.

In order to examine the mechanism causing isolation in our CELC limiters, we calculate the power transmitted, reflected, and absorbed in the CELC array at both low power (0 dBm) and high power (+30 dBm). The calculated results are shown in Fig. 7(a) (for 0 dBm) and (b) (for +30 dBm).

Fig. 7(a) illustrates that for low power, a substantial amount is transmitted near the resonance frequency (over 50%) with over 40% absorption. Fig. 7(b) illustrates that for high power, the

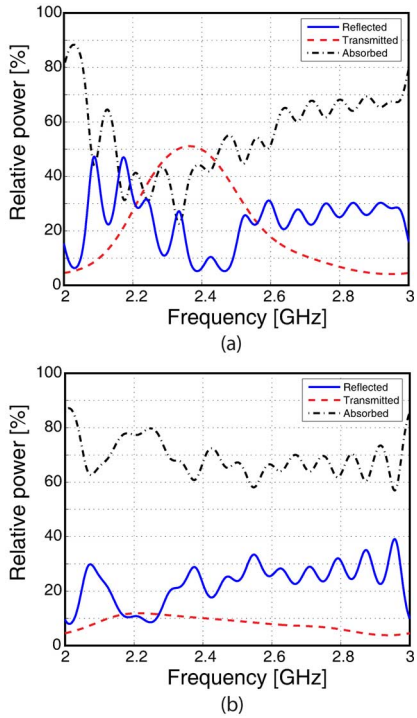

Fig. 7. Power analysis for the CELC array at different $P_{\rm in}$ levels. (a) $P_{\rm in} = 0$ dBm. (b) $P_{\rm in} = +30$ dBm. The changes in transmission and absorption indicate that the majority of the incident power is being absorbed at high $P_{\rm in}$.

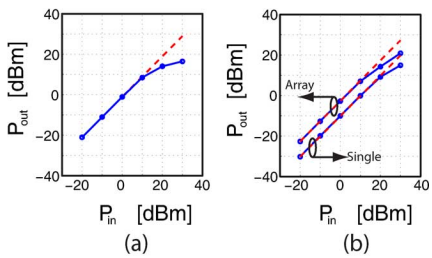

Fig. 8. *(color online)* Experimental $P_{\rm out}$ versus $P_{\rm in}$ curves for the CPW circuit limiter, single CELC, and array of CELCs. In both subplots, the dashed red curve represents flat transmission at all $P_{\rm in}$ levels with a given insertion loss representing a generic linear device. In both subplots, the solid blue data are the measured data for a particular limiter. (a) $P_{\rm out}$ versus $P_{\rm in}$ curve for CPW limiter. (b) $P_{\rm out}$ versus $P_{\rm in}$ for CELC surfaces. Single CELC data and CELC array data are indicated. The higher insertion loss of the single CELC is easily seen by the vertical shift of the single CELC curves, while the array of CELCs has insertion loss similar to that of the CPW limiter.

transmission drops to under 12%, while the absorption increases to over 70%. This demonstrates that the isolation is largely due to increased absorption rather than increased reflection.

Using our experimental data, we calculate the $P_{\rm out}$ versus $P_{\rm in}$ curves for the traditional CPW limiter, our single CELC limiter, and our array CELC limiter. The results are presented in Fig. 8(a) (CPW limiter), (b) (single CELC limiter), and (c) (array CELC limiter).

It is seen from this data that the threshold power $P_{\rm t}$ for the CPW limiter [Fig. 8(a)] and the array of CELCs [Fig. 8(c)] is approximately the same. The CPW limiter has slightly higher isolation at high power levels than the array CELC limiter, as shown previously, but the overall performance is similar. Our array CELC has similar performance to a traditional CPW circuit-based RF limiter. However, it is implemented as a 2-D sheet of arbitrary size and can be fully extended to a volumetric limiter, as it is implemented using metamaterials. This allows the construction of a sheet or volumetric limiter to protect sensitive components without requiring circuit connections.

V. Conclusion

In conclusion, we have demonstrated the feasibility of using metamaterials to construct RF limiter sheets. We have fabricated and tested a CELC-based RF limiter metamaterial that exhibits < 3 dB minimum insertion loss at low power with a maximum isolation of 9.3 dB. The unit cells can function individually to provide over 10 dB isolation or can be combined into an effective medium to provide low insertion loss with over 6 dB of isolation at the resonant frequency and a 3-dB isolation bandwidth of 18%. This letter demonstrates that metamaterials can be used to implement practical, useful technologies through the inclusion of nonlinear effects.

References

[1] D. R. Smith, W. J. Padilla, D. C. Vier, S. C. Nemat-Nasser, and S. Schultz, "Composite medium with simultaneously negative permeability and permittivity," *Phys. Rev. Lett.*, vol. 84, no. 18, pp. 4184–4187, May 2000.

[2] R. W. Ziolkowski, "Propagation in and scattering from a matched metamaterial having a zero index of refraction," *Phys. Rev. E*, vol. 70, no. 4, p. 046608, Oct. 2004.

[3] D. Schurig, J. J. Mock, B. J. Justice, S. A. Cummer, J. B. Pendry, A. F. Starr, and D. R. Smith, "Metamaterial electromagnetic cloak at microwave frequencies," *Science*, vol. 314, no. 5801, pp. 977–980, 2006.

[4] N. Landy, S. Sajuyigbe, J. J. Mock, D. R. Smith, and W. J. Padilla, "Perfect metamaterial absorber," *Phys. Rev. Lett.*, vol. 100, p. 207402, 2008.

[5] S. Gu, J. P. Barrett, T. H. Hand, B.-I. Popa, and S. A. Cummer, "A broadband low-reflection metamaterial absorber," *J. Appl. Phys.*, vol. 108, p. 064913, 2010.

[6] I. V. Shadrivov, S. K. Morrison, and Y. S. Kivshar, "Tunable split-ring resonators for nonlinear negative-index metamaterials," *Opt. Exp.*, vol. 14, no. 20, pp. 9344–9349, 2006.

[7] D. Huang, E. Poutrina, and D. R. Smith, "Analysis of the power dependent tuning of a varactor-loaded metamaterial at microwave frequencies," *Appl. Phys. Lett.*, vol. 96, no. 10, p. 104104, 2010.

[8] I. V. Shadrivov, A. B. Kozyrev, Y. S. van der Weide, W. Daniel, and Kivshar, "Tunable transmission and harmonic generation in nonlinear metamaterials," *Appl. Phys. Lett.*, vol. 93, no. 16, p. 161903, 2008.

[9] D. Huang, A. Rose, E. Poutrina, S. Larouche, and D. R. Smith, "Wave mixing in nonlinear magnetic metacrystal," *Appl. Phys. Lett.*, vol. 98, p. 204102, 2011.

[10] A. R. Katko, S. Gu, J. P. Barrett, B.-I. Popa, G. Shvets, and S. A. Cummer, "Phase conjugation and negative refraction using nonlinear active metamaterials," *Phys. Rev. Lett.*, vol. 105, p. 123905, 2010.

[11] T. H. Hand, J. Gollub, S. Sajuyigbe, D. R. Smith, and S. A. Cummer, "Characterization of complementary electric field coupled resonant surfaces," *Appl. Phys. Lett.*, vol. 93, p. 212504, 2008.